Pergamon

Available online at www.sciencedirect.com

SCIENCE DIRECT®

Cement and Concrete Research 33 (2003) 841–849

CEMENT AND CONCRETE RESEARCH

Flexural performance of ring-type steel fiber-reinforced concrete

O.C. Choi[a], C. Lee[b,*]

[a]*Department of Architectural Engineering, Soong-Sil University, Seoul, 156-743, Republic of Korea*
[b]*Department of Architectural Engineering, Chung-Ang University, Ansung 456-756, Republic of Korea*

Received 29 January 2001; accepted 9 December 2002

Abstract

Steel fiber-reinforced concrete (SFRC) with randomly dispersed, short straight steel fibers hardly fails by fiber yielding, and the postpeak behavior is governed by mechanisms related to fiber pullout. It would be more desirable if more fracture energy could be consumed by fiber yielding at failure. It has been experimentally demonstrated in this research that SFRC with the ring-type steel fibers failed by more energy consuming mechanisms other than fiber pullout. Consequently, significant improvements in flexural toughness were obtained as compared to that of SFRC with conventional straight steel fibers.

Keywords: Bending strength; Bond, Fiber reinforcement; Fracture toughness

1. Introduction

Stress systems produced in concrete by external loads (compression, tension, flexure, or multiaxial) give rise to a process of propagation and interconnection of microcracks in cementitious materials [1–4]. Reinforcement of concrete with short, randomly distributed steel fibers leads to improvements in the tensile strength and tensile and compressive ductility of the material [5–9]. This is due to the tendency of propagating microcracks in cementitious matrices to be arrested or deflected by fibers [1,2,7,10,13]. While the prepeak behavior and maximum tensile strength of the composite material depends on local bond characteristics at the fiber–matrix interface, the postpeak behavior is dominated by an average bond behavior in pullout action of fibers bridging the critical crack. Fiber–matrix interfacial bond strength is provided by a combination of adhesion, friction, and mechanical interlocking [11].

The primary advantage in using SFRC is its high performance in flexure. In most cases, steel fibers are pulled out after debonding rather than being ruptured under tensile stress. It is, however, more desirable if more energy can be consumed by fiber yielding. This can only be achieved if sufficiently long steel fibers embedded in concrete can resist the pullout forces. As longer fibers are used with higher aspect ratio, problems may arise associated with mixing, random distribution of fibers, and their economical applicability. In practice, therefore, the practical range of diameters and aspect ratios of steel fibers is limited, so that the mechanical performance of commercially available straight steel fibers will depend upon their fiber pullout resistance.

To overcome the limitations that traditional straight steel fibers have, ring-type steel fibers are used in this research. While the mechanical performance of traditional straight steel fibers relies on the fiber–matrix interfacial bond strength, ring-type steel fibers are mainly designed to mobilize fiber yielding rather than fiber pullout. Experimental verifications are presented showing the effectiveness and superiority with regards to flexural behavior of ring-type steel fibers over traditional straight steel fibers. Investigated for ring-type steel fiber-reinforced concrete (RSFRC) are characteristics of flexural performance, toughness indices, influential parameters, and influence in comparison with SFRC reinforced with straight hooked-end steel fibers (SHSFRC).

2. Experimental program

Flexural tests are conducted according to ASTM C 78 to determine characteristics of behavior of RSFRC. SHSFRC beams are also tested for comparison.

Ring diameter, fiber diameter, and fiber content are selected as the main experimental parameters. Ring-type steel fibers were produced with five different ring diameters (20, 30, 40, 50, and 60 mm) and four different fiber

* Corresponding author. Tel.: +82-31-670-3346; fax: +82-31-675-6489.
E-mail address: cdlee@cau.ac.kr (C. Lee).

0008-8846/03/$ – see front matter
doi:10.1016/S0008-8846(02)01093-1

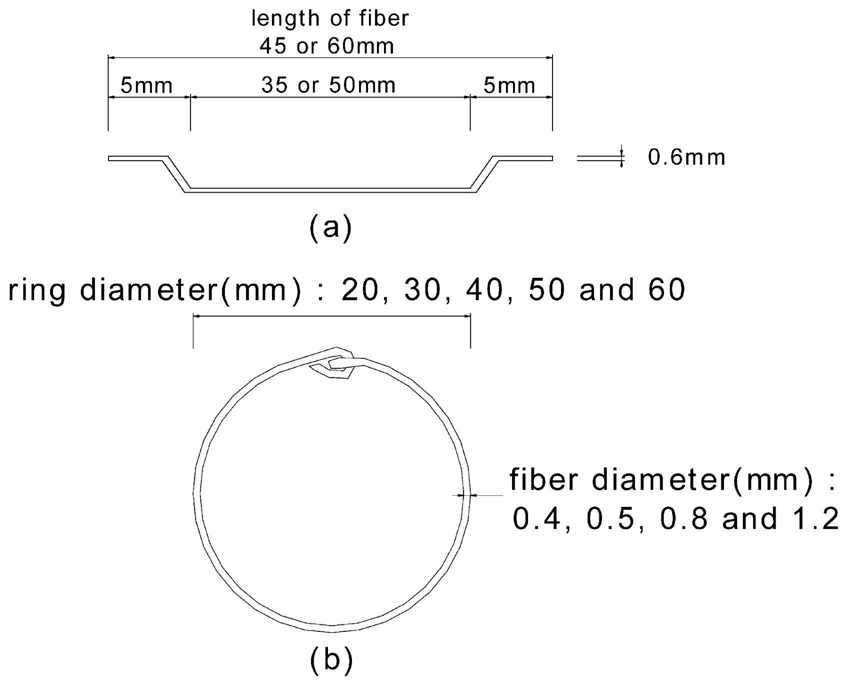

Fig. 1. Fiber geometry: (a) hooked-end straight steel fiber, (b) ring-type steel fiber.

diameters (0.4, 0.5, 0.8, and 1.2 mm). They were employed in two different fiber volume contents (0.20% and 0.40%). Parameter combinations were tried to find the best geometry of ring-type steel fibers for the most efficient performance minimizing the total number of specimens.

Since the ring-type steel fibers were not commercially available, they were produced from pieces of cold-drawn wires by manufacturing machine. The average tensile strength of the three wires used for the ring-type steel fibers was 4120 MPa.

Commercially available hooked-end straight steel fibers were used. Fibers with 0.6 mm diameter and 45 and 60 mm length were used for comparison tests in which three different fiber volume contents, 0.20%, 0.40%, and 0.80%, were applied. The fiber geometries of typical ring-type and hooked-end steel fibers are shown in Fig. 1.

Concrete mix was designed to achieve 33.9 MPa compressive strength at 28 days. Use was made of ordinary Portland cement, river sand, and a crushed limestone coarse aggregate with 15 mm maximum grain size. Cement, fine aggregate, and coarse aggregate were mixed in the proportions of 1:1.92:2.36 by weight. The water-to-cement ratio was kept constant at 0.48. The content of fibers in the mix was measured in their mass per unit volume. The preparation of all the mixes was essentially similar.

Firstly, the abovementioned mix was prepared, where upon the fibers were uniformly fed into the mix by hand. Minor balling was observed during mixing although good workability of RSFRC without dosing any superplasticizer would have been expected. Occasional manual dispersion may be required in some cases. Test specimens were compacted on a vibrating table. All specimens were cured at 95% RH for 72 h and then demolded. After 56 days of air curing in the laboratory environment at 23 ± 2 °C, all specimens were tested in flexure within 63 days of age.

Flexural tests under third-point loading were performed in accordance with ASTM C 78. The testing system was a computer-controlled closed-loop servo-hydraulic universal testing machine. The test arrangement is shown in Fig. 2. In the middle of test, a yoke, rather than a stroke method, is used as proposed in ASTM C 1080 to eliminate extraneous

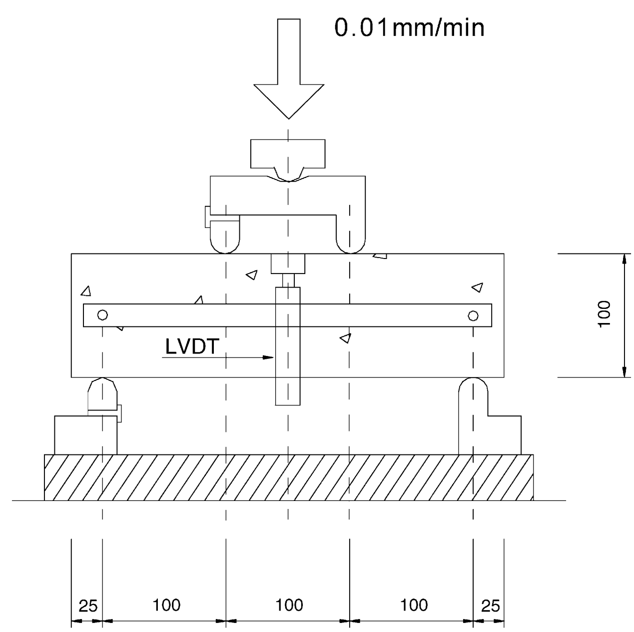

Fig. 2. Flexural test arrangement (in mm).

deflections at the supports [14]. Load and deformation data were recorded during the tests and stored by the data acquisition system for processing at a later stage. The flexural tests were run under displacement control at a rate of 0.01 mm/min. The tests were continued until midspan deflection reached 2.0 mm, which was equivalent to span/150 at the center of the beam specimen. During the computation of toughness, the average tangent stiffness of the specimens from the yoke tests was used to correct the stiffness of the stroke tests.

3. Test results and discussion

3.1. Failure mode

Tables 1 and 2 present the test results of SHSFRC and RSFRC, respectively. All specimens failed by flexure. However, unlike the pulling out of fibers in the SHSFRC specimens under increasing loadings, those that bridged a critical section in the RSFRC specimens successively broke. Typical load–deflection curves of the RSFRC specimens are presented in Fig. 3. Load and deflections increased almost proportionally up to the first crack load. One major crack occurred in the central part of the specimen. On average, only a marginal load increase was observed at modulus of rupture (MOR). The subsequent flexural behavior in the postpeak region fell into one of the following patterns: (i) sudden drop and then gradual decrease in load-carrying capacity and (ii) sudden drop, which was gradually recovered, followed by gradual decrease in load-carrying capacity. The failure behavior of SHSFRC followed one of the two patterns as revealed by Fig. 3a. Different load–deflection curves of RSFRC, however, were observed compared to those of SHSFRC (see Fig. 3b). After sudden drop following prepeak load, resistance gradually increased in some specimens. The marginal drops in the load were due to the rupture of individual fibers crossing the critical section. Postpeak resistance was usually recovered after the marginal drop when some of the fibers crossing the critical section were again mobilized to resist flexural tensile stresses by yielding to rupture. As observed, the failure of postpeak behavior of RSFRC in this mode suggests that the continuous fracturing sound of ring-

Table 1
Test results of SHSFRC

Specimen label[a]	Fiber volume content (%)	First crack load (kN)	Displacement at first crack load (mm)	Maximum load (kN)	Average toughness indices		
					I_5	I_{10}	I_{20}
DH150645A	0.2	–	–	–	3.3	5.7	9.8
DH150645B		13.6	0.064	13.6			
DH300645A	0.4	16.5	0.077	16.5	2.7	5.7	10.4
DH300645B		–	–	–			
DH600645A	0.8	13.1	0.062	16.0	5.1	10.4	20.5
DH600645B		16.3	0.076	16.3			
DH150660A	0.2	14.0	0.065	14.0	4.6	8.5	15.7
DH150660B		11.8	0.055	12.6			
DH300660A	0.4	14.3	0.067	14.3	3.8	7.2	14.0
DH300660B		15.8	0.073	15.8			
DH600660A	0.8	15.2	0.071	16.6	5.9	12.7	21.2
DH600660B		–	–	–			

[a] Specimen label: NT C FD RD R: NT = fiber type: DH, FR; C = fiber volume content: 0.2%, 0.4%, and 0.8%; FD = fiber diameter: 0.4, 0.5, 0.6, 0.8, and 1.2 mm; RD = ring diameter or fiber length: 20, 30, 40, 50, and 60 mm; R = replication: A, B.

Table 2
Test results of RSFRC

Specimen label[a]	Fiber volume content (%)	First crack load (kN)	Displacement at first crack load (mm)	Maximum load (kN)	Average toughness indices		
					I_5	I_{10}	I_{20}
NFA[b]	–	13.6	0.130	13.7	–	–	–
NFB[b]		13.8	0.140	13.8			
FR150420A	0.2	10.8	0.051	10.8	4.4	7.8	14.4
FR150420B		12.5	0.058	12.5			
FR150520A		12.3	0.058	12.3	4.4	7.9	13.6
FR150520B		–	–	–			
FR150430A		14.1	0.066	15.4	4.0	8.3	16.2
FR150430B		12.0	0.056	13.0			
FR150530A		16.7	0.078	16.7	3.8	6.7	13.6
FR150530B		12.5	0.058	12.5			
FR150440A		14.2	0.066	14.2	4.6	9.0	17.9
FR150440B		17.5	0.082	17.5			
FR150540A		–	–	–	2.9	5.4	10.1
FR150540B		17.0	0.080	17.0			
FR300420A	0.4	14.9	0.070	14.2	4.8	9.2	17.4
FR300420B		14.1	0.066	14.9			
FR300520A		14.8	0.069	14.8	4.0	6.3	11.3
FR300520B		16.3	0.076	16.3			
FR300430A		13.4	0.063	18.8	4.6	9.0	20.0
FR300430B		13.3	0.062	13.3			
FR300530A	0.4	16.7	0.078	16.7	4.9	9.5	18.6
FR300530B		12.8	0.060	13.0			
FR300440A		14.4	0.067	19.2	4.3	8.6	19.0
FR300440B		13.4	0.063	15.7			
FR300540A		15.3	0.072	16.9	4.3	8.6	19.7
FR300540B		14.9	0.070	19.7			
FR150840A	0.2	14.8	0.069	14.8	3.9	6.8	12.9
FR150840B		14.6	0.068	14.6			
FR150850A		12.5	0.058	12.5	5.4	7.5	11.9
FR150850B		12.0	0.056	12.0			
FR150860A		9.1	0.043	9.1	4.2	7.3	14.6
FR150860B		–	–	–			
FR300840A	0.4	15.4	0.072	15.4	3.9	7.4	14.6
FR300840B		14.6	0.068	14.6			
FR300850A		–	–	–	3.5	5.5	11.2
FR300850B		13.6	0.064	13.6			
FR300860A		16.5	0.077	19.7	2.6	4.8	7.5
FR300860B		13.3	0.062	14.0			
FR301240A		13.9	0.065	13.9	3.9	7.3	12.3
FR301240B		14.1	0.066	14.1			
FR301250A		11.6	0.054	11.6	5.7	7.3	9.3
FR301250B		15.6	0.073	15.6			
FR301260A		12.7	0.060	12.7	2.9	4.9	9.2
FR301260B		10.7	0.050	10.7			

[a] Specimen label: NT C FD RD R: NT = fiber type: DH, FR; C = fiber volume content: 0.2%, 0.4%, and 0.8%; FD = fiber diameter: 0.4, 0.5, 0.6, 0.8, and 1.2 mm; RD = ring diameter or fiber length: 20, 30, 40, 50, and 60 mm; R = replication: A, B.

[b] NFA and NFB = specimens with plain concrete.

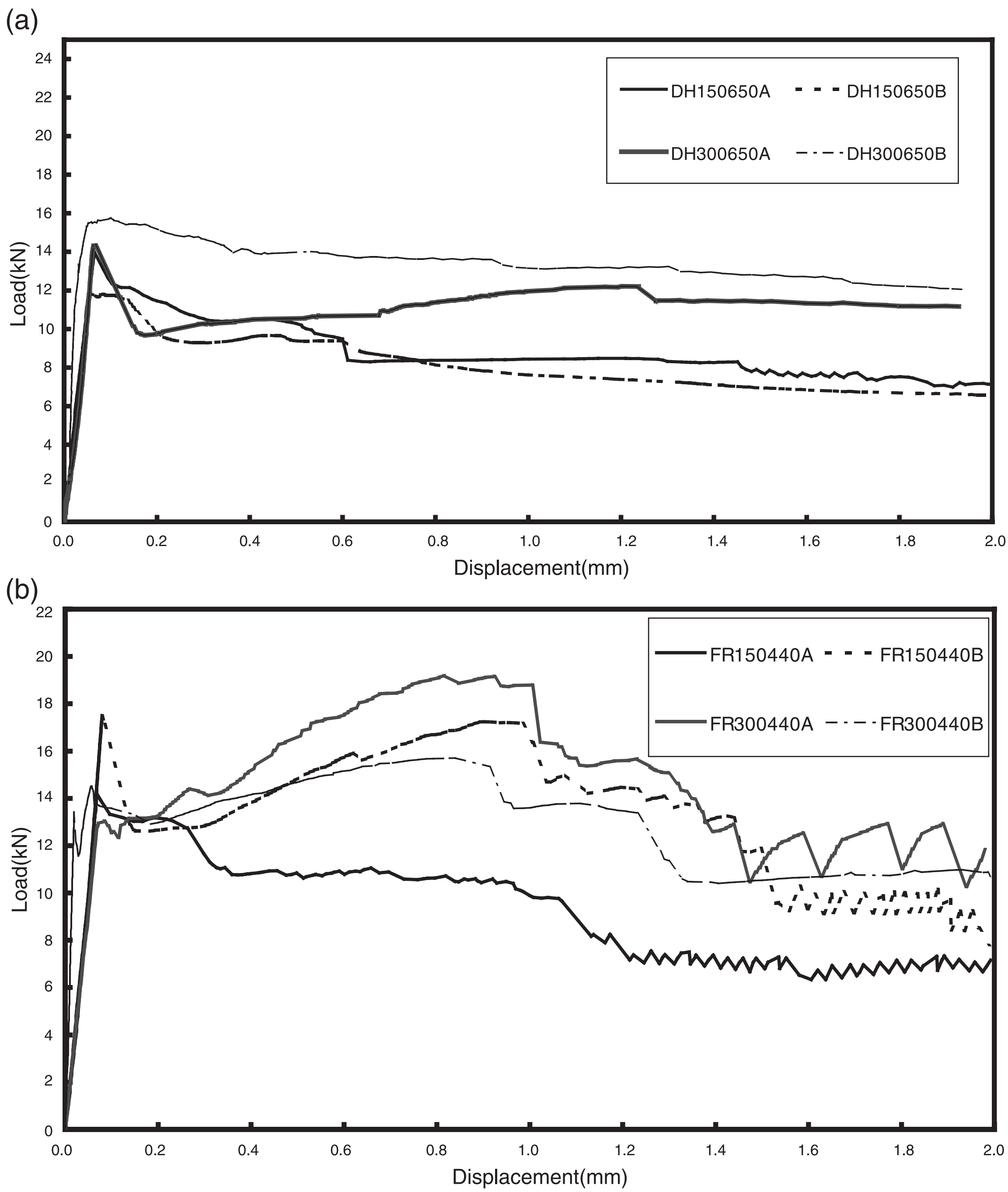

Fig. 3. Typical load–deflection curves of SFRC: (a) SHSFRC with fiber diameter of 0.6 mm and fiber length of 50 mm, (b) RSFRC with fiber diameter of 0.4 mm and ring diameter of 40 mm.

type steel fibers and marginal fluctuation of resisting load were due to the gradual tensile rupture of ring-type steel fibers. These fluctuations of postpeak load resistance were more clearly observed for RSFRC than for SHSFRC.

After a series of tests, the specimens of SHSFRC and RSFRC were intentionally opened to examine the failure surface at the critical section. Two completely different types of fiber failure were identified as shown in Fig. 4. As observed in previous studies [11–13], failure of SHSFRC takes place mostly through fiber pullout after progressive fiber–matrix debonding. Some fibers also exhibited straightened ends that were originally in hooked configuration. In contrast, no fiber pullout was observed for RSFRC. Instead, it was found that some fibers had ruptured after yielding at the fractured section. In addition, fracture of concrete surrounding embedded ring-type steel fibers occurred at this section.

Experimentally observed flexural failure mechanisms of RSFRC were involved with three different types: fiber rupture after yielding, cone-type concrete fracture, and

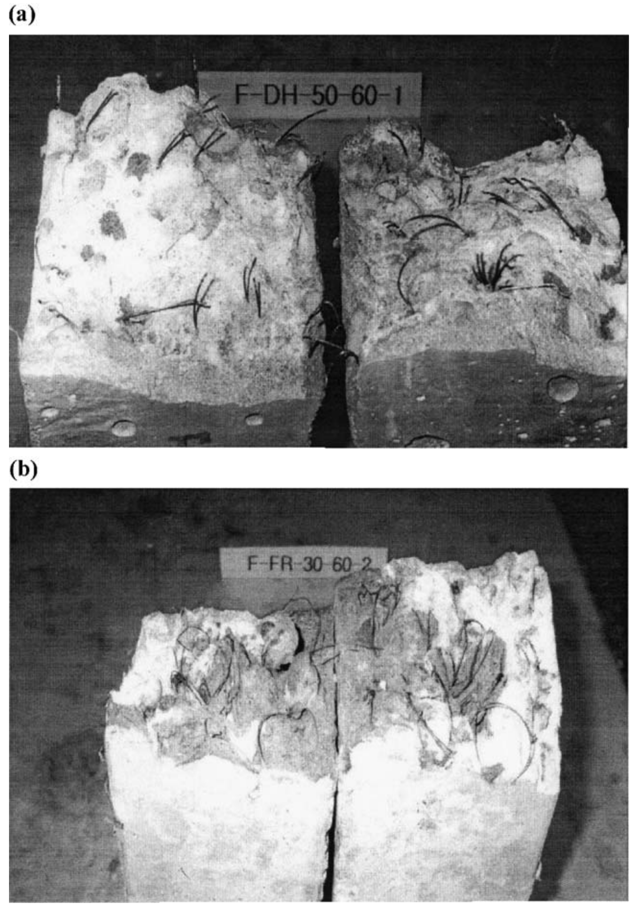

Fig. 4. Typical fractured surfaces of SHSFRC and RSFRC beams: (a) SHSFRC, (b) RSFRC.

separation between ring-type steel fibers and concrete matrix as illustrated in Fig. 5.

3.2. First crack loads

First crack load as defined in ASTM C 1018 was measured. According to ASTM C 1018, the first crack load is the point on the load–deflection curve at which the form of the curve becomes nonlinear. First crack loads from experiment for both specimens of SHSFRC and RSFRC were observed to be marginally higher than those of plain concrete. On average, there seemed to be basically no difference in first crack load between SHSFRC and RSFRC. The deflections of midspan at the first crack loads ranged from 0.043 to 0.082 mm for RSFRC and from 0.055 to 0.077 mm for SHSFRC.

3.3. Toughness of SHSFRC

The most beneficial effect of adding steel fibers to plain concrete would be to increase the toughness of concretes [2,3,5–7]. This can be estimated by calculating toughness indices. The method recommended in ASTM C 1018 is used for this purpose. Toughness of SHSFRC, as reflected by such indices, was found improved at higher fiber contents and larger aspect ratios reported in international literatures.

3.3.1. Effect of fiber contents

Regardless of fiber aspect ratio, increasing fiber content from 0.20% to 0.40% has little influence on the toughness indices of I_5, I_{10}, and I_{20} as shown in Fig. 6. However, toughness indices increased on average about 73% as fiber contents increased from 0.20% to 0.80%.

3.3.2. Effect of aspect ratio

Values of toughness index in Fig. 6, especially for I_{20}, increased when aspect ratio was raised from 75 (=45/0.6 mm) to 100 (=60/0.6 mm). The average values for I_{20} for 45-mm-long fibers were 9.77, 10.36, and 20.5, whereas the averages were 15.67, 14.09, and 21.60 for 60-mm-long fibers for 0.20%, 0.40%, and 0.80%, respectively.

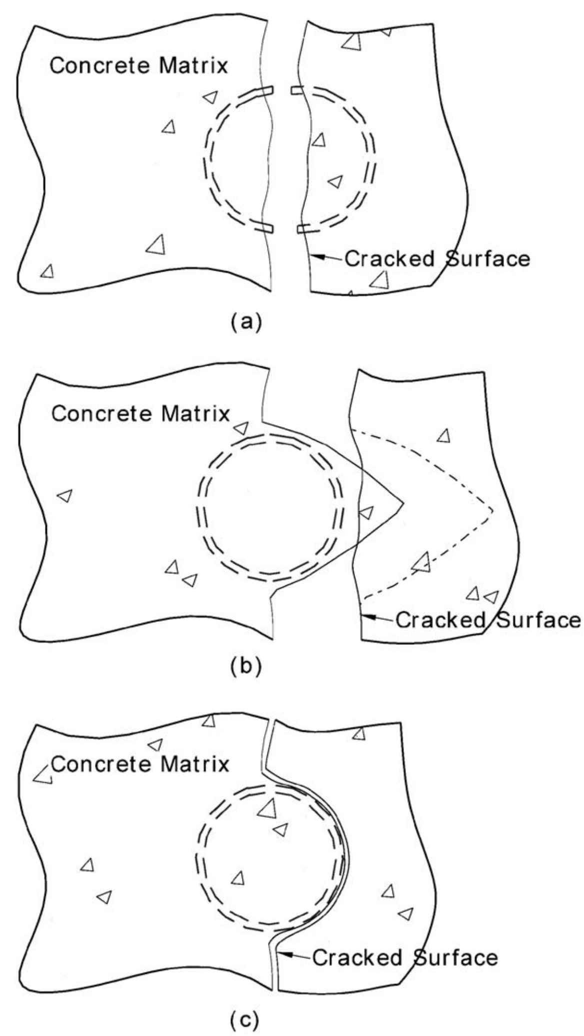

Fig. 5. Three types of failure patterns: (a) Fiber rupture after yielding, (b) cone-type concrete fracture, (c) separation between ring-type steel fibers and concrete matrix.

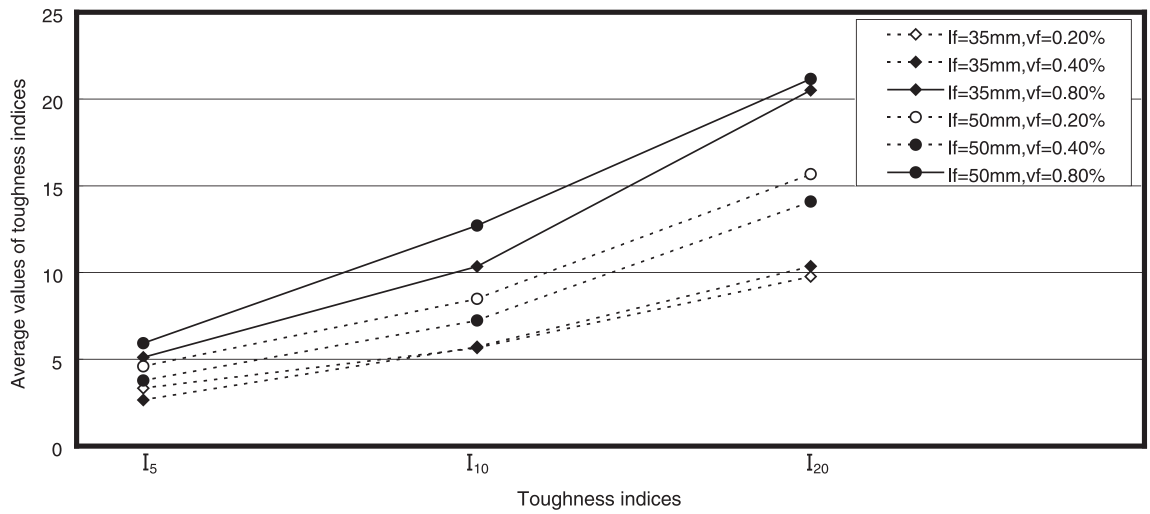

Fig. 6. Average values of toughness indices of SHSFRC (v_f = fiber volume content and l_f = fiber length).

3.4. Toughness of RSFRC

Toughness indices of RSFRC were affected by fiber contents, ring diameter, and fiber diameter. Detailed observations are given in the following.

3.4.1. Effect of fiber contents

Fig. 7 shows that for ring diameters of 30 mm or less, toughness increases marginally as fiber volume content is doubled from 0.20% to 0.40%. The observed average values of toughness index for I_5, I_{10}, and I_{20} for fiber volume contents of 0.20% were 4.0, 7.5, and 14.2, respectively, while the averages for 0.40% were 4.4, 8.3, and 16.7, respectively. Usually, as fiber content increases, the number of fibers crossing the fractured section increases and more favorable failure mechanisms can be mobilized, leading to a higher toughness. This was demonstrated experimentally for SHSFRC. When fiber content was raised from 0.20% to 0.40%, toughness index I_{20} was increased with respect to the average value of 72% for the two different aspect ratio cases (see Fig. 6).

3.4.2. Effect of ring diameter

To assess the relations between toughness indices and ring diameter, test results were evaluated from RSFRC with ring diameters of 20, 30, 40, 50, and 60 mm and with fiber diameters of 0.4, 0.5, 0.8, and 1.2 mm. The effect of ring diameter on I_{20} is shown in Fig. 8. In this figure, values of toughness index at I_{20} are plotted as a function of ring diameter for each fiber diameter.

The results show that as the ring diameter increases from 20 to 40 mm, the values of I_{20} toughness index increase in general. However, a further increase in diameter from 40 to 60 mm leads to a decline in toughness index. An optimum ring diameter appears to be approximately 40 mm for the maximum aggregate size of 15 mm used in this study. This observation indicates that ring diameter clearly influences

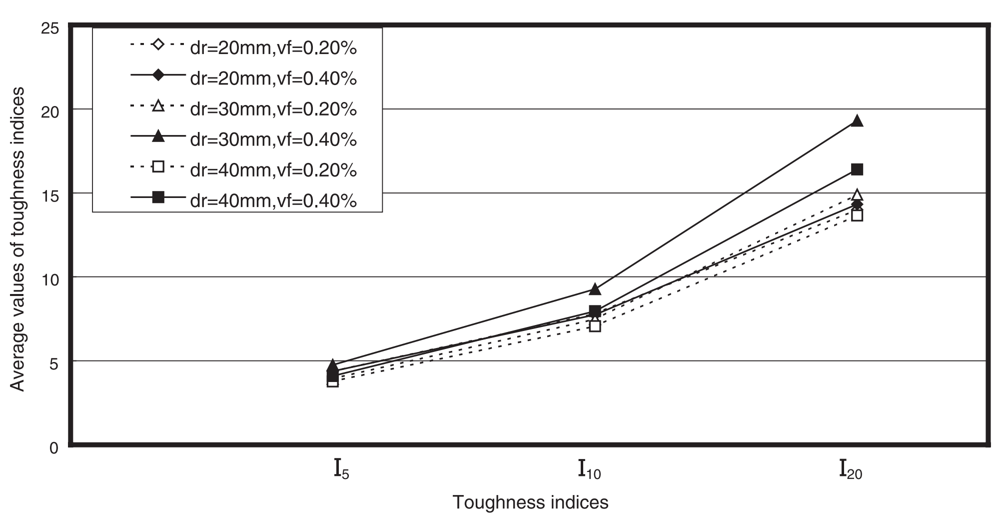

Fig. 7. Average values of toughness indices of RSFRC (v_f = fiber volume content and d_r = ring diameter).

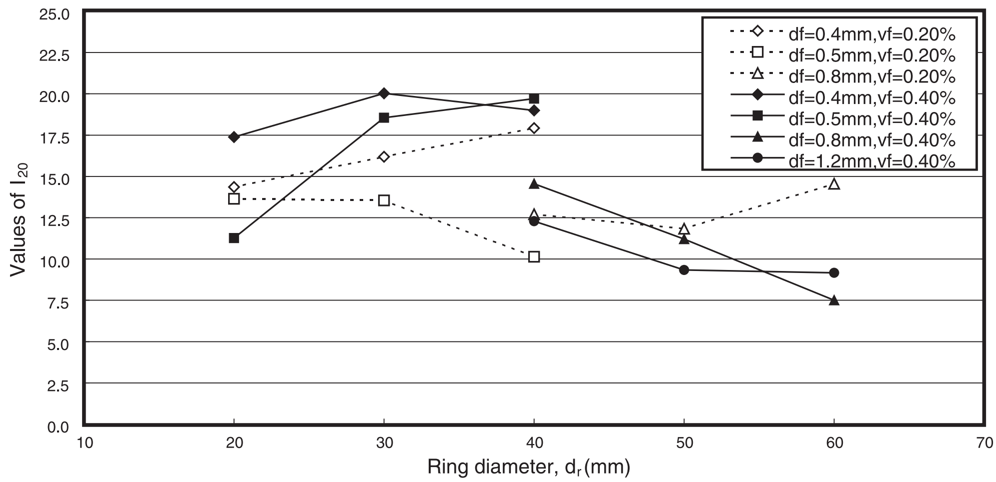

Fig. 8. Effect of ring diameter on the values of toughness index I_{20} (d_f = fiber diameter and v_f = fiber volume content).

the performance of RSFRC, and an optimum ring diameter will exist for a given mix.

3.4.3. Effect of fiber diameter

For a given fiber content, the number of fibers increases as fiber diameter decreases. Thus, more fibers will cross the fractured section at failure and toughness will increase accordingly. As fiber diameters increase, values of toughness index decrease. This trend is most clearly observed for I_{20}, regardless of the fiber contents as shown in Fig. 9.

At the same fiber content, the number of fibers would be increased by four times as the fiber diameter reduces to half. When fiber diameter is reduced from 1.2 to 0.4 mm in this study, the number of fibers intersecting with the fractured plane is increased nine times nevertheless. Values of I_{20} increased approximately from 10.26 to 18.80 on average for RSFRC with fiber content of 0.40% as shown in Fig. 9. This shows that fiber diameter is one of the key parameters affecting the toughness index of RSFRC. Those RSFRC with smaller fiber diameter are expected to have better toughness indices unless failure of fibers occur by rupture at a too low stress level before concrete cone-type failure occurs due to insufficient sectional area of fibers.

4. Comparison of toughness indices between RSFRC and SHSFRC

Comparisons of flexural performance in terms of values of toughness index between RSFRC and SHSFRC are made. For the comparison, results of RSFRC with ring diameter of 30 mm and results of SHSFRC with hooked-end straight steel fibers with fiber length of 60 mm are used. For both cases, fiber content of 0.20% and 0.40% are used. Comparisons are made for these two different cases since these two resulted in best toughness for two different types of steel fibers.

Fig. 10 illustrates effectiveness of RSFRC compared to SHSFRC in increasing flexural toughness. Toughness indices I_{20} of RSFRC for fiber volume content of 0.20% and 0.40% are 16.2 and 20.2, respectively, and those for

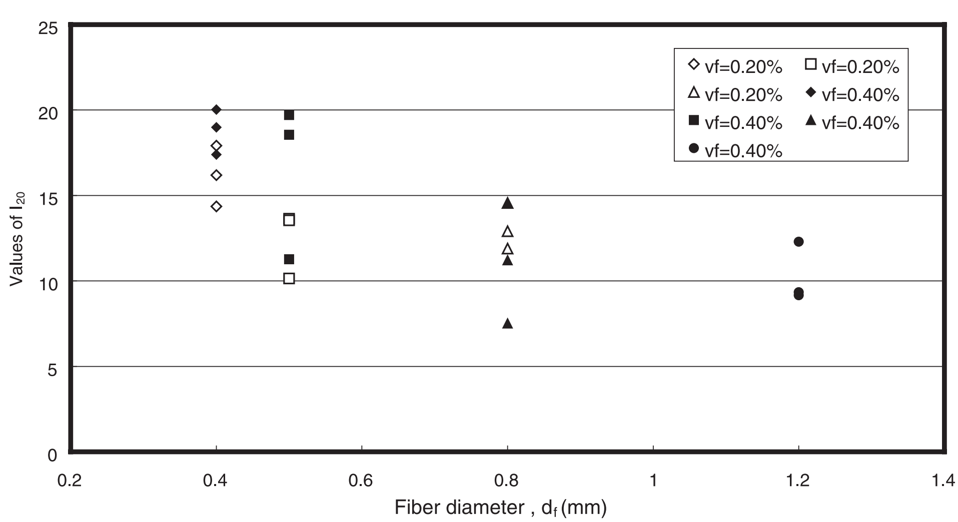

Fig. 9. Effect of fiber diameter on the values of toughness index I_{20} (v_f = fiber volume content).

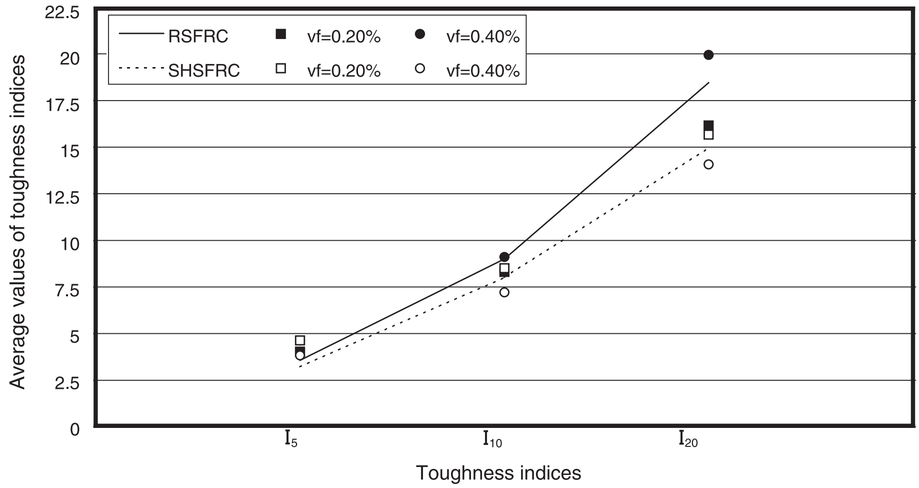

Fig. 10. Comparison of toughness index values between RSFRC and SHSFRC (v_f = fiber volume content).

SHSFRC are 15.7 and 14.1, respectively. Regarding the toughness index of I_{20}, RSFRC has 22% larger toughness on average compared to that of SHSFRC.

In Fig. 11, relative increases of toughness over the overall averaged toughness of SHSFRC including both fibers of length 45 and 60 mm are given for RSFRC with ring-type steel fibers of ring diameter 30 mm. The average toughness indices of I_{20} are 12.2 and 12.7 for fiber content of 0.20% and 0.40% that can be compared to the values of 16.2 and 20.0 for RSFRC, respectively. It can be seen that for all toughness indices, RSFRC has better toughness than those of SHSFRC. At I_{20}, RSFRC was observed to be 45% more effective than SHSFRC over the average toughness.

For the same volume contents, RSFRC showed better performance under flexure than SHSFRC, although some variances with limited number of specimens were observed in their improvements. Although better performance of RSFRC can be expected in terms of flexural toughness, further study is needed to find the optimum size for fiber diameter relative to ring diameter.

5. Conclusions

The following conclusions are drawn from this study.

1. Investigation of the fractured surface of the RSFRC after completion of flexural tests showed that there are three different types of the failure mechanisms: the yielding and rupturing of ring-type steel fibers, cone-type fracture of the matrix concrete surrounding the embedded ring-type steel fibers, and the separation of concrete around the ring-type steel fibers. Failure mechanisms of RSFRC do not involve pullout mechanism as in conventional SFRC with straight steel fibers.

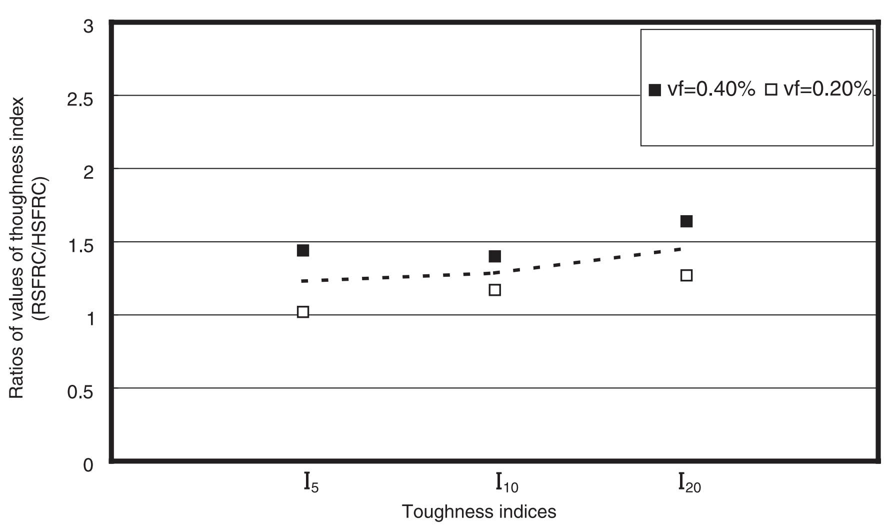

Fig. 11. Ratio of toughness index values of RSFRC to those of SHSFRC at I_{20} (v_f = fiber volume content).

2. The first crack loads were marginally higher than those of plain concrete, and basically there were no differences in magnitude of first crack loads between RSFRC and SHSFRC.
3. Influential factors with respect to flexural toughness of RSFRC were experimentally observed to be the ring diameter, diameter of steel fiber, and fiber content. Values of toughness index were marginally influenced as the amount of fiber volume contents was doubled from 0.20% to 0.40%. The ring diameter for the best interlocking between fibers and aggregate appears to be approximately 40 mm for the maximum aggregate size of 15 mm. It seems that there exists an optimum ring diameter for a given RSFRC mixture. As fiber diameter became smaller, values of toughness index increased. The trends were observed for I_{20} regardless of the fiber volume content of 0.20% or 0.40%.
4. Comparisons between RSFRC and SHSFRC showed that RSFRC performs 45% better on overall average than SHSFRC in terms of values of toughness index at I_{20}. When the best results from RSFRC and SHSFRC were compared, RSFRC still exhibited 22% higher toughness index value at I_{20} than SHSFRC.

References

[1] V.S. Gopalaratnam, S.P. Shah, Softening response of plain concrete in direct tension, Am. Conc. Inst. 82 (3) (1985) 310–323.

[2] S. Diamond, A. Bentur, On cracking in concrete and fiber reinforced cements, in: S.P. Shah (Ed.), Application of Fracture Mechanics to Cementitious Composites, NATO-ARW, Kluwer Academic Publishers, Netherlands, 1984, pp. 87–140.

[3] V.S. Gopalaratnam, S.P. Shah, Failure mechanisms and fracture of fiber reinforced concrete, Proceedings of Fiber Reinforced Concrete Symposium, November, ACI, Baltimore, MD, 1986, pp. 1–26.

[4] N.G. Shrive, Compression testing and cracking of plain concrete, Mag. Concr. Res. 135 (122) (1983) 27–39.

[5] S.P. Shah, V. Rangan, Fiber reinforced concrete properties, Am. Concr. Inst. 68 (2) (1971) 126–135.

[6] P.S. Mangat, Tensile strength of steel fiber reinforced concrete, Cem. Concr. Res. 6 (2) (1976) 245–252.

[7] D. Fanella, A. Naaman, Stress–strain properties of fiber reinforced mortar in compression, Am. Concr. Inst. 82 (4) (1985) 475–483.

[8] R. Jindal, Shear and moment capacities of steel fiber reinforced concrete beams, Fiber Reinforced Concrete, Am. Concr. Inst., SP-81 (1983) 1–16.

[9] R.N. Swamy, S.A. Al-Taan, Deformation and ultimate strength in flexure of reinforced concrete beams made with steel fiber concrete, Am. Concr. Inst. 78 (5) (1981) 310–323.

[10] R. Craig, J. McConnell, H. Germann, N. Dib, F. Kashani, Behavior of reinforced fibrous concrete columns, Am. Concr. Inst., SP-81 (1981) 69–105.

[11] A. Bentur, Interfaces in fiber reinforced cements, Proc. Mater. Res. Soc. Symp. 114 (1998) 133–261.

[12] A. Naaman, S.P. Shah, Pull-out mechanism in steel fiber reinforced concrete, Am. Soc. Civil Eng. 102 (8) (1976) 1537–1549.

[13] P. Soroushian, Z. Bayasi, Fiber-type effects on the performance of steel fiber reinforced concrete, Am. Concr. Inst. Mater. J. 88 (2) (1991) 129–134.

[14] N. Banthia, J. Trottier, Test methods for flexural toughness characterization of fiber reinforced concrete: some concerns and a proposition, Am. Concr. Inst. Mater. J. 92 (1) (1995).